

Catalysis Science & Technology

Accepted Manuscript



This is an *Accepted Manuscript*, which has been through the Royal Society of Chemistry peer review process and has been accepted for publication.

Accepted Manuscripts are published online shortly after acceptance, before technical editing, formatting and proof reading. Using this free service, authors can make their results available to the community, in citable form, before we publish the edited article. We will replace this *Accepted Manuscript* with the edited and formatted *Advance Article* as soon as it is available.

You can find more information about *Accepted Manuscripts* in the [Information for Authors](#).

Please note that technical editing may introduce minor changes to the text and/or graphics, which may alter content. The journal's standard [Terms & Conditions](#) and the [Ethical guidelines](#) still apply. In no event shall the Royal Society of Chemistry be held responsible for any errors or omissions in this *Accepted Manuscript* or any consequences arising from the use of any information it contains.

Cite this: DOI: 10.1039/c0xx00000x

www.rsc.org/xxxxxx

ARTICLE TYPE

Peroxonioibium(V) catalyzed selective oxidation of sulfides with hydrogen peroxide in water: a sustainable approach

Sandhya Rani Gogoi,^a Jeena Jyoti Boruah,^a Gargi Sengupta,^a Gangutri Saikia,^a Kabirun Ahmed,^a Kusum Kumar Bania^a and Nashreen S. Islam^{*a}

5 Received (in XXX, XXX) Xth XXXXXXXXXX 20XX, Accepted Xth XXXXXXXXXX 20XX

DOI: 10.1039/b000000x

An efficient and eco-compatible route for the selective oxidation of a variety of thioethers to the corresponding sulfoxide or sulfone with 30% aqueous H₂O₂ in water, using newly synthesized peroxonioibium (pNb) complexes as catalysts, is described. The catalysts formulated as, 10 Na₂[Nb(O₂)₃(arg)].2H₂O (arg = arginate) (**NbA**) and Na₂[Nb(O₂)₃(nic)(H₂O)].H₂O (nic = nicotinate) (**NbN**) have been synthesized from the reaction of sodium tetraperoxonioibate with 30% H₂O₂ and the respective organic ligand in aqueous medium, and comprehensively characterized by elemental analysis, spectral studies (FTIR, Raman, ¹H NMR, ¹³C NMR and UV-Vis), EDX and TGA-DTG analysis. Density functional method (DFT) has been used to investigate the structure of the synthesized pNb 15 complexes. The catalysts are physiologically safe, and can be reused for at least up to six reaction cycles without losing their activity or selectivity. The oxidation is chemoselective for sulfides or sulfoxides leaving a C=C or alcoholic moiety unaffected. The developed methodologies, apart from being high yielding and straightforward, are completely free from halogen, organic co-solvent, or co-catalyst.

1 Introduction

20 Chemoselective oxidation of organic sulfides represents one of the most fundamentally important reactions in the domain of organic chemistry which is fascinating from both chemical as well as biological perspectives.¹ The practical utility of sulfoxides and sulfones as high value commodity chemicals and their 25 versatility as precursors for gaining access to a variety of chemically and biologically active molecules including drugs and chiral auxiliaries, have been adequately highlighted in the literature.^{1a,d,e,2}

A number of highly promising new catalytic strategies for 30 selective sulfoxidation using various oxidants have been developed in the past few years based on transition metal catalysts, particularly those from groups 4-7 in their highest oxidation states such as titanium,³ vanadium,⁴ chromium,⁵ iron,⁶ molybdenum,⁷ tungsten^{7c,8} and rhenium⁹. Many of the available 35 methods however, rely upon the use of toxic and volatile organic solvents, harmful oxidants or require harsh reaction conditions, which lower the practical importance of otherwise efficient oxidation catalysts. Thus, notwithstanding the enormous progress in the development of catalytic protocols to achieve selective 40 oxidation of sulfides, the important criterion of ecological sustainability is still a challenging issue to address. Sustainability of a chemical transformation is mainly governed by the solvent, reagents and catalysts used, in addition to the work up procedure

employed.^{6b} In view of the current ecological concerns, the 45 demand for catalytic oxidation processes that use benign solvent, green oxidants and reagents which co-produce only innocuous waste, seems to have intensified.^{7c,8,10} Out of the multitude of available organic oxidants, aqueous 30% H₂O₂ has been recognized as the best waste-preventing terminal oxidant for 50 reasons of high oxygen content, cost, safety and easy handling.^{10c-e,11}

Water holds great promise as an alternative to traditional 55 organic solvents as it is inexpensive, safe and non-volatile, with unique redox stability and high heat capacity.¹² Although, traditionally, water is referred to as ‘the universal solvent’, in organic synthesis water has been treated as a contaminant mainly due to the concern regarding solubility.^{12a} However, since the ‘on water’ approach pioneered by Sharpless,^{12b} which demonstrated that solubility is not a requisite to reactivity, and that many 60 organic transformations can be performed efficiently in aqueous solvent, there has been phenomenal progress in the field of water based organic synthesis.^{12b,13} This also necessitated the development of water-tolerant catalysts to support such transformations. There are reports, although very limited, on 65 metal-catalyzed sulfoxidation reaction in aqueous medium.^{6a, 7a,10h,14} Very recently, Chakroborty and co-workers reported a surfactant based Mo catalyst for selective sulfoxidation of a variety of sulfides in aqueous medium with 40% H₂O₂.^{7a}

In the recent past, we have successfully developed a set of new recoverable heterogeneous catalysts based on polymer immobilized peroxotungsten (pW) and peroxomolybdenum (pMo) complexes which displayed excellent stability, selectivity and efficiency with respect to yield, TON and TOF for the oxidation of diverse range of thioethers and dibenzothiophene by H_2O_2 under very mild conditions.^{7b,8a} Few of these supported catalysts also effectively catalyzed the oxidative bromination of a variety of activated aromatics at ambient temperature and near neutral pH.¹⁵ Furthermore, a number of dimeric as well as macromolecular water soluble peroxo compounds of vanadium and tungsten prepared by us, could serve as stoichiometric oxidants of organic bromides and sulfides in aqueous organic medium.¹⁶

In our continuing endeavours devoted to developing newer catalyst and methodologies for oxidations under environmentally acceptable reaction conditions, in the present work we have aspired to design new peroxometal based catalytic systems for selective sulfoxidation using H_2O_2 as oxidant in aqueous medium. We selected peroxoniobium (pNb) system as an ideal candidate for our study for a variety of reasons. Most importantly, Nb has been reported to be non-toxic to animal, with LD 50 values in several thousand mg/kg body weight in contrast to its lighter group 5 element vanadium, which is known to be moderately toxic.¹⁷ Catalysis by pNb compounds is a field of growing interest.¹⁸ The pNb species generated in situ in presence of H_2O_2 , have been shown to catalyze, oxidation of sulfides,^{18c-g} alcohol,^{18h} as well as epoxidation of alkene^{18a,b,i}. For example, Egami *et al.* used Nb(salan) complexes to catalyze the asymmetric epoxidation of allylic alcohol with urea-hydrogen peroxide adduct with good selectivity.^{18a} However, catalytic potential of discreet synthetic heteroligand pNb complexes, as oxidation catalyst have rarely been investigated.

Proper choice of the co-ligand is an important prerequisite in order to obtain stable and well defined peroxometallates. Moreover, the coordinating ligand has been shown to have a dramatic effect on the reactivity of peroxometallates (pM) which enabled the activity of pM complexes as stoichiometric or catalytic agent to be fine-tuned with ligands.¹⁹ For the present investigation, since our focus was to develop physiologically harmless catalysts, we have chosen nicotinic acid (also known as niacin) and an amino acid, arginine as potential co-ligands. These ligands possess carboxylate functional for easy attachment to Nb(V) centre, in addition to N-donor site. Carboxylate anion has been known to be excellent co-ligand for stabilising pNb species.²⁰ Consequently, a host of pNb complexes have been reported in recent years possessing ligands with carboxylate

moiety.²⁰

On the other hand, although scores of publications, including from our laboratory have dealt with the synthesis and characterization of peroxometal complexes of V,^{16a-d,21} Mo²² and W^{16e,21f,23} with amino acid or nicotinic acid as co-ligand,²⁴ as far as we are aware arginine and nicotinic acid have not so far been used to obtain heteroleptic pNb complex in the solid state. Apart from being biologically relevant, these ligands are reasonably inexpensive, water soluble, and commercially available.

We report herein, the catalytic activity of a pair of newly synthesised pNb complexes for the controlled oxidation of sulfides with H_2O_2 in aqueous medium, in terms of selectivity, yield, reusability and sustainability, to obtain sulfoxide or sulfone.

2 Results and discussion

2.1 Synthesis and Characterization

A reasonably straightforward synthetic route has been established to obtain a pair of stable and water soluble pNb complexes with arginine or niacin as co-ligand. The procedure is based on the reaction of sodium tetraperoxoniobate with 30% H_2O_2 and the respective co-ligand, in an aqueous medium at near neutral pH. Synthesis of soluble niobium (V) compounds is considered to be rather challenging owing to very low solubility of the common Nb containing starting materials.^{18d} In the present study, water soluble $\text{Na}_3[\text{Nb}(\text{O}_2)_4] \cdot 13\text{H}_2\text{O}$ has been used as precursor complex, which was prepared by reported method.¹⁸ⁱ The maintenance of pH of ca. 6 was found to be essential for the formation of the triperoxoniobium species and its stabilisation by the chosen organic ligands, occurring in their anionic form, leading to the isolation of the complexes **NbA** and **NbN**. The procedure included other requirements such as maintenance of temperature at $\leq 4^\circ\text{C}$ and limiting water to that contributed by 30% H_2O_2 . The compounds were observed to be stable in the solid state for several weeks when stored dry in closed container at $< 30^\circ\text{C}$.

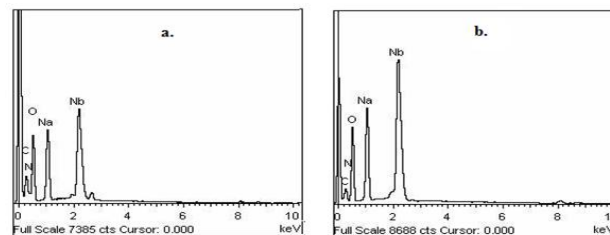


Fig. 1 EDX spectra of (a) **NbA** and (b) **NbN**.

Table 1 Analytical data for the synthesized peroxo-niobium complexes

Complexes	% found from elemental analysis/ EDX (Theoretical %)					% O_2^{2-} content (Theoretical %)
	C	H	N	Nb	Na	
$\text{Na}_2[\text{Nb}(\text{O}_2)_3(\text{arg})] \cdot 2\text{H}_2\text{O}$	16.29	3.76	12.46	21.01 ^a	11.14	21.71
	16.15		12.76	20.84	10.47	
	(16.21)	(3.83)	(12.61)	(20.92)	(10.36)	
$\text{Na}_2[\text{Nb}(\text{O}_2)_3(\text{nic})(\text{H}_2\text{O})] \cdot \text{H}_2\text{O}$	18.41	1.99	3.55	23.52 ^a	11.63	24.54
	18.37		3.61	23.57	11.66	
	(18.32)	(2.03)	(3.56)	(23.64)	(11.70)	

^aDetermined by AAS.

The elemental analysis data (Table 1), for each of the title compounds indicated the presence of three peroxide groups and one ancillary ligand, arginine or niacin per Nb(V) centre which could be fitted with the formulation, $\text{Na}_2[\text{Nb}(\text{O}_2)_3(\text{arg})] \cdot 2\text{H}_2\text{O}$ and $\text{Na}_2[\text{Nb}(\text{O}_2)_3(\text{nic})(\text{H}_2\text{O})] \cdot \text{H}_2\text{O}$. Energy dispersive X-ray spectroscopic analysis (EDX) clearly showed the presence of Nb, Na, C, N and O in the complexes (Fig. 1). Data obtained on the composition of the compounds from EDX analysis were in good agreement with elemental analysis values (Table 1). Despite many attempts, it was not possible to obtain crystals of the compounds large enough for an X-ray crystal structure. The compounds were diamagnetic in nature as was evident from the magnetic susceptibility measurements, in conformity with the presence of Nb in its +5 oxidation state.

2.1.1 IR and Raman spectral studies

The complexes **NbA** and **NbN** displayed distinctive spectral pattern in the IR region [Fig. S1 (ESI†)]. The Raman spectra of the compounds complemented the IR spectra, confirming the presence of co-ordinated peroxy and the respective co-ligand in each of them. The significant general features of IR and Raman spectra are summed up in Table 2. The Raman spectra for the complexes are presented in Fig. 2.

A triperoxy niobium species with triangularly bonded peroxy group has been reported to exhibit a diagnostic IR pattern with three $\nu(\text{O}-\text{O})$ bands in the $800\text{--}880\text{ cm}^{-1}$ region.^{18d,25} The IR and Raman spectra of each of the compounds **NbA** and **NbN** enabled clear identification of three sharp absorptions representing the characteristic $\nu(\text{O}-\text{O})$ modes of peroxy group, in addition to the $\nu_{\text{asym}}(\text{Nb}-\text{O}_2)$ and $\nu_{\text{sym}}(\text{Nb}-\text{O}_2)$ vibrations, as has been expected, in the $870\text{--}810$ and $500\text{--}600\text{ cm}^{-1}$ region, respectively.

On the basis of the available reported data pertaining to metal compounds with co-ordinated amino acid and niacin as ligands, empirical assignments could be derived for the IR and Raman bands observed for the catalysts **NbA** and **NbN**.

Table 2 Experimental and theoretical infrared and Raman spectral data (in cm^{-1}) for the compounds, **NbA** and **NbN**^a

Assignment			NbA	NbN	
$\nu(\text{O}-\text{O})$	IR	Exp.	846(m), 813(s)	822(sh), 847(m), 811(s)	
		Calc.	837, 865, 889	807, 872	
	R	Exp.	823(sh), 857(sh)	847(s), 817(sh), 867(sh)	
		Calc.	806, 853, 879	813, 828, 876	
	$\nu_s(\text{Nb}-\text{O}_2)$	IR	Exp.	547(s)	547(s)
		Calc.	528	523	
R		Exp.	538(s)	542(s)	
$\nu_{\text{as}}(\text{Nb}-\text{O}_2)$	IR	Exp.	592(m)	593(sh)	
	Calc.	604	605		
	R	Exp.	567(sh)	571(sh)	
$\nu_{\text{as}}(\text{COO}^-)$	IR	Exp.	1636(s)	1625(s)	
	Calc.	1615	1649		
	R	Exp.	1630(vw)	1627(sh)	
$\nu_s(\text{COO}^-)$	IR	Exp.	1406(m)	1388(s)	
	Calc.	1375	1378		
	R	Exp.	1410(vw)	1393(sh)	
Calc.	1403	1335			

^as, strong; m, medium; vw, very weak; sh, shoulder.

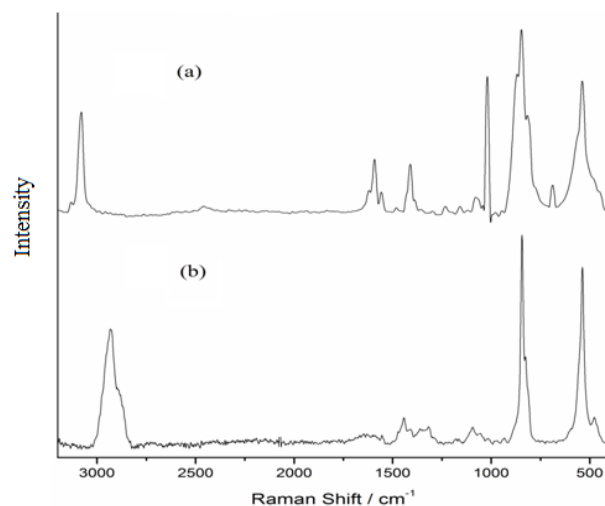


Fig. 2 Raman spectra of (a) **NbN** and (b) **NbA**.

The IR spectra of arginine, as well as of arginato-metal complexes have been reported previously.²⁷ In the spectrum of free arginine $\nu_{\text{as}}(\text{COO}^-)$ and $\nu_s(\text{COO}^-)$ modes are observed at 1606 and 1425 cm^{-1} , respectively with $\Delta\nu = 181$ [$\Delta\nu = \nu_{\text{as}}(\text{COO}^-) - \nu_s(\text{COO}^-)$]; whereas, in case of the complex **NbA**, the corresponding absorptions appeared at 1636 cm^{-1} and 1406 cm^{-1} , respectively. The shift of $\nu_{\text{as}}(\text{COO}^-)$ to higher frequency and that of $\nu_s(\text{COO}^-)$ to a lower frequency compared to the free ligand values, with an increase in the $\Delta\nu$ ($= 230\text{ cm}^{-1}$), is typical of unidentate co-ordination of carboxylate group.^{26a} In the Raman spectrum of the compound, weak intensity bands representing $\nu_{\text{as}}(\text{COO}^-)$ and $\nu_s(\text{COO}^-)$ vibrations have been located at 1630 and 1410 cm^{-1} , respectively. The $\nu(\text{C}-\text{H})$ occurred as an intense peak at 2934 cm^{-1} in the Raman spectrum in contrast to its presence as a weak band in the IR. Two bands typical of $\nu(\text{NH}_2)$ are observed at 3352 and 3288 cm^{-1} in the free ligand spectrum.^{27a} A new peak appeared at 3193 cm^{-1} in the spectrum of the complex **NbA** indicative of co-ordinated amino group.^{27a} However, the other absorptions representing $\nu(\text{N}-\text{H})$ could not be assigned with certainty owing to their overlapping with $\nu(\text{OH})$ modes of lattice water, appearing as a broad band in the $3500\text{--}3300\text{ cm}^{-1}$ region.

In the catalyst **NbN**, the presence of carboxylato bonded niacin has been clearly demonstrated by its IR and Raman spectra (Table 2). A number of reports are available on IR spectral characterization of metal complexes containing co-ordinated niacin.^{26c,e,f} Moreover, the IR and Raman spectra of NIA have been thoroughly investigated by Kumar and co-workers and others.^{26d} Solid sodium nicotinate exhibits major carboxylate IR bands at 1620 and 1416 cm^{-1} respectively for $\nu_{\text{as}}(\text{COO}^-)$ and $\nu_s(\text{COO}^-)$.^{26f} The positions of $\nu_{\text{as}}(\text{COO}^-)$ and $\nu_s(\text{COO}^-)$ stretchings in both IR and Raman spectra of **NbN** and the corresponding $\Delta\nu$ ($= 237\text{ cm}^{-1}$) value provide clear evidence of unidentate co-ordination of a non-protonated carboxylato group to the metal atom. Furthermore, a significantly less intense aromatic $\nu(\text{CC})$ band at 1568 cm^{-1} depicts monodentate coordination of carboxylate group to Nb.^{26g} Since the $\nu(\text{CC})$ mode, $\nu(\text{CN})$ absorption as well as pyridine ring vibrations at 1476 , 1016 and 940 cm^{-1} , respectively do not undergo any positive shift relative to the respective free ligand values, coordination via pyridine ring nitrogen can safely be ruled out.^{26c} The presence of water

molecule in the complex was apparent from the observance broad and intense $\nu(\text{OH})$ bands in the 3500 to 3400 cm^{-1} region. Further confirmation for the presence of co-ordinated water in the compound was obtained from the consistent appearance of a moderate intensity signal at 769 cm^{-1} attributable to rocking mode of water.²⁸ The intense band appearing at 3077 cm^{-1} in the Raman spectrum has been ascribed to $\nu(\text{CH})$ vibration.

2.1.2 Electronic spectral studies

Close analogy was observed between the UV-Vis spectral patterns of compounds **NbA** and **NbN**, recorded in aqueous solution. The spectra exhibited two bands at *ca.* 280 and *ca.* 325 nm attributable to peroxy to metal charge transfer bands, as has been observed in case of other reported triperoxoniobium(V) complexes.^{20f,i,29}

2.1.3 ¹H and ¹³C NMR Studies

In Tables 3 and 4, relevant ¹H and ¹³C NMR resonances for the catalysts are listed along with those of the free ligand for comparison. Crucial structural information regarding the complexes, including the co-ordination mode of the ligand to the Nb atom, as well as their stability in solution have been gathered from the complete analysis of the NMR spectra. The major NMR resonances were interpreted according to available literature data. The ¹H-NMR spectra in D₂O have shown the expected integration and peak multiplicities [Fig. S2 (ESI†)].

The spectral pattern of the pNb complex with arginine as co-ligand resembled closely the spectrum of the free ligand, by exhibiting 4 major peaks at 3.52, 3.11, 1.74 and 1.59 ppm.³⁰ The spectrum of the complex however, showed distinct upfield shift of all the resonances relative to the free ligand indicating co-ordination of the ligand to the metal centre.³⁰ Similar observations were made previously in case of metal compounds containing complexed amino acid.^{30,31}

Table 3 ¹H Chemical shifts for ligands and heteroligand peroxy-niobate complexes

Compound	Chemical shift (ppm) ^a				
	H-2	H-3	H-4	H-5	H-6
Arginine	3.76	1.89	1.66	3.23	-
NbA	3.52	1.74	1.59	3.11	-
Niacin	8.97	-	8.68	7.93	8.76
NbN	8.82	-	8.13	7.40	8.49

^aSee Fig. 4 for the atomic numbering.

The ¹³C chemical shift induced by coordination has been widely utilized as a convenient means to understand bonding pattern of ancillary ligands in peroxy-metal complexes.³² The ¹³C NMR spectrum of the free arginine in D₂O, displays typical resonance for carboxylate carbon atom at 183.17 ppm, in addition to the five other well resolved peaks corresponding to carbon atoms C(2) to C(6).³⁰ The spectrum of **NbA**, on the other hand displayed the carboxylate resonance at lower field of 215.45 ppm thus testifying to the existence of complexed carboxylate

Table 4 ¹³C NMR chemical shift for ligands and triperoxoniobium complexes, **NbA** and **NbN**

Compound	Chemical shift (ppm) ^a					
	Carboxylate Carbon	C ₂	C ₃	C ₄	C ₅	C ₆
Arginine	183.17	55.59	31.64	24.51	41.02	56.81
NbA	215.45	54.59	30.28	23.99	40.64	56.83
Niacin	168.25	143.04	135.49	42.49	126.94	45.89
NbN	210.78	149.06	137.69	42.46	128.76	50.51

^aSee Fig 4 for the atomic numbering.

The substantial downfield shift relative to free carboxylate, with $\Delta\delta$ ($\delta_{\text{complex}} - \delta_{\text{free carboxylate}}$) \approx 32 ppm indicated strong metal-ligand interaction as has been reported earlier in case of some other peroxy metal carboxylate complexes.^{33,7b} The guanidyl C resonance along with the resonances of alkyl groups (C-5 and C-4) showed very little shift, whereas the resonances of α -CH and β -CH₂ groups are shifted to higher field by *ca.* 1 ppm [Fig. S3 (a) (ESI†)]. These results indicated the co-ordination of carboxylate and amino groups of the ligand to the niobium centre and are consistent with observations made in case of other reported arginine containing metal compounds.³⁰

The ¹H as well as ¹³C NMR spectra of nicotinic acid in D₂O has been studied and reported by Khan and co-workers under varying pH conditions.³⁴ A ¹H NMR pattern typical of a nicotinate anion was observed with four well-resolved resonances in the spectrum of the compound **NbN**.³⁴ As expected for nicotinate anion the spectrum showed characteristic up field shift of each of the four resonances corresponding to the aromatic protons H(2) to H(6), relative to the zwitterionic free ligand values [Fig S2 (a) (ESI†)].^{30b}

The ¹³C spectrum provided further persuasive evidence in support of the presence of nicotinate anion in the compound **NbN** by displaying resonances for ring carbon atoms in the region expected for nicotinate anion.³⁴ The peak attributable to metal bound carboxylate carbon, as in the case of **NbA**, appeared at a considerably lower field of 210.78 ppm, compared to the carboxylate resonance of the free nicotinic acid [Fig S3 (b) (ESI†)].^{33,7b} Occurrence of the carboxylate carbon as a singlet in the spectrum of each of the catalysts, **NbA** and **NbN**, indicated a single carbon environment for complexed carboxylate.³³ Thus the results of the NMR analysis evidenced for the presence of only one complex species in solution in each case. It is therefore apparent that catalysts did not hydrolyze and retained their solid state structure in solution.

2.1.4 TGA-DTG Analysis

The TGA-DTG plots illustrated in Fig. 3 for the catalysts **NbA** and **NbN** showed that the compounds gradually undergo multistage decomposition on heating up to a temperature of 700 °C. Interestingly, the compounds do not explode on heating although, majority of the known pNb compounds have been reported to decompose explosively on heating.^{20b,f,35}

The first stage of decomposition for **NbA** [Fig 3 (a)] occurs in the temperature range of 78 – 102 °C, with the liberation of the lattice water from the complex. The corresponding weight loss of 8.9% is in good agreement with the value of 8.1% calculated for

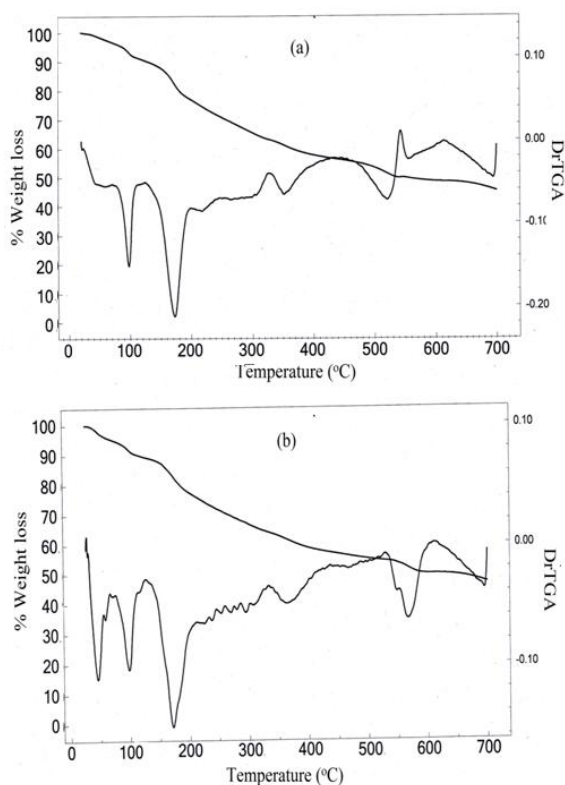


Fig. 3 TGA-DTG plot of (a) **NbA** and (b) **NbN**.

two molecules of water of crystallization. The next decomposition stage is in the temperature range of 157-189 °C attributable to loss of peroxy groups from the complexes with weight loss of 18.8%. As the observed weight loss is slightly less than the expected value, it is likely that part of the oxygen is retained with niobium to form oxoniobium species, as has been observed previously in case of neat as well as heteroligand pNb complexes.^{20b,f,35} A further increase in temperature leads to continuous degradation of the arginine ligand up to a final decomposition temperature of 700 °C. The total weight loss which occurred during the overall decomposition process was evaluated to be 54.3%, which agree well with the theoretically calculated value of 54.6%, for the loss of the components viz., water molecule, co-ordinated peroxide, and the co-ligand, assuming that four of the ligand oxygen atoms being retained to form the oxoniobate species as the final degradation product.

It is notable that the thermogram for **NbN** [Fig. 3 (b)] displayed two step dehydration process in the temperature range of 45-105 °C, providing conclusive evidence for the presence of outer sphere as well as co-ordinated water molecules in the compound, consistent with the formula assigned. The decomposition step occurring at relatively higher temperature between 90 to 105 °C, after the initial liberation of the outer sphere water molecule in the temperature range of 45-70 °C, is attributable to the loss of the co-ordinated water molecule. The observed total weight loss of 9.8% corresponding to the two steps combined, is close to the calculated value of 9.2% for the release of two molecules of water from the complex. After the dehydration, the thermal behaviour of catalysts **NbA** and **NbN** are quite similar. The compound **NbN** undergoes continuous

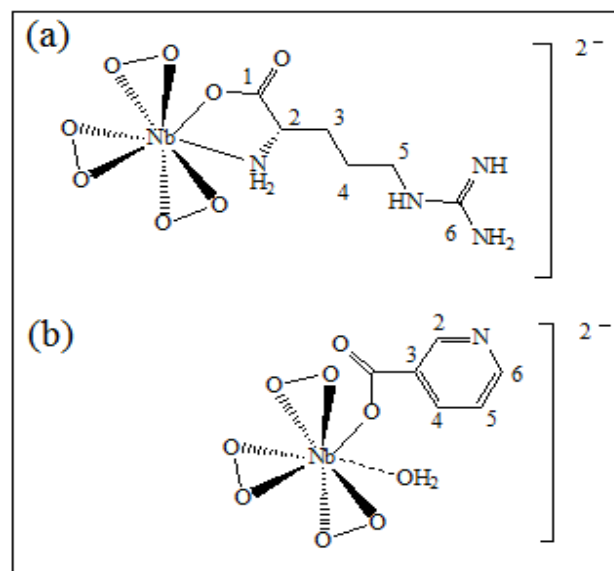


Fig. 4 Proposed structure of (a) **NbA** and (b) **NbN**.

degradation with loss of peroxide in the temperature range of 158 – 189 °C analogous to compound **NbA**, followed by the loss of the niacin ligand up to the final temperature of 700 °C. The residue remaining after the complete degradation of each of the pNb compounds, was found to be oxoniobate species as indicated by the IR spectral analysis which showed the typical $\nu(\text{Nb}=\text{O})$ stretching and was devoid of absorptions attributable to peroxy and the respective co-ligands of the starting complex.

The above results are consistent with the proposed structures of the compounds **NbA** and **NbN** shown schematically in Fig. 4. The structure of **NbA** shows the Nb atom displaying a co-ordination number of eight, surrounded by the three peroxo groups and the arginate ligand bonded via its unidentate carboxylate group and the amino group. The structure of **NbN** includes nicotinate anion occurring as a unidentate ligand bonded to the Nb centre through the carboxylate group, the side-on bound peroxo groups and a co-ordinated water molecule completing eight-fold co-ordination around Nb.

2.1.5 Theoretical investigation

In order to verify the feasibility of the proposed structures, Density Functional Theory (DFT)³⁶ calculations were performed on the two niobium complexes at B3LYP/LANL2DZ level of theory. The initial structures of the two complexes were modeled based on the experimental data related to the compounds (FTIR, Raman, ¹³C and ¹H NMR, TGA and elemental analysis). The optimized geometries of the two niobium complexes are presented in Fig. 5. In both the complexes the coordination polyhedron around the niobium atom is a dodecahedron as observed in majority of the reported pNb complexes.^{18d, 20f}

In case of **NbA**, the central metal atom (Nb) is co-ordinated to six oxygen atoms belonging to three η^2 -peroxo groups, in addition to one oxygen from carboxylate group and a N (amino) atom from the deprotonated arginate ligand. One of the bidentate peroxo groups is in *trans* position to the co-ligand whereas, the other two are in *cis* configuration. The co-ordination sphere of complex **NbN** comprises of niobium atom surrounded

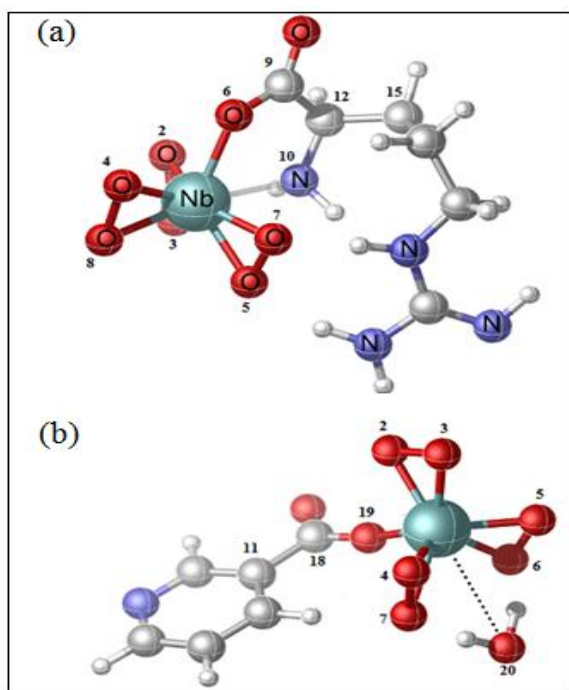


Fig. 5 Optimized geometry of (a) **NbA** (b) **NbN**. The numerical numbers represents the labeling of the atoms as in Table 5.

by seven oxygen atoms contributed by three η^2 -peroxo groups and one from the unidentate carboxylato group of the nicotinate ligand. The eighth co-ordination site is satisfied by water molecule which is weakly bonded to the central atom, as has been observed previously by Djordjevic *et al.* in case of nicotinate containing peroxomolybdenum complex.²⁴ Thus the structure of **NbN** can be described as a distorted octahedron with one of the axial distances slightly longer. For both the complexes the coordination distances are within the range characteristic of heteroleptic peroxo complexes of niobium(V).^{20f} The geometrical parameters (bond angle and bond length) obtained from DFT calculations are depicted in Table 5. The Nb-O(peroxo) bond lengths are within the range of 1.977 to 2.086 Å whereas, the (O-O) distances range from 1.526 to 1.533 Å. The Nb-O (carboxylate) bond distances in **NbA** and **NbN** are 2.162 Å and 2.138 Å, respectively. The Nb-N bond distance in **NbA** is 2.370 Å. The geometrical parameters obtained from our theoretical calculation correlated well with the reported crystallographic parameters pertaining to other heteroleptic triperoxo niobate complexes with coordination environment comprising of N, O- or O-donor co-ligands.^{18d,20e,f} The small differences observed between the experimental and calculated geometrical parameter are expected, as the ground state geometries were obtained in the gas phase by full geometry optimization.

We have further calculated the vibrational frequencies for the optimized geometries of the compounds and compared the data obtained with the experimentally determined frequencies as illustrated in Table 2. The calculated IR and Raman spectra for the two complexes are found to simulate well with the experimental ones. The small deviations between the calculated

Table 5 Selected bond lengths (in Å) and bond angles (in degree) for the two complexes calculated at B3LYP/LANL2DZ level of theory

Structural Index ^a	NbA	Structural Index ^a	NbN
Nb-O2	2.072	Nb-O2	2.047
Nb-O3	2.008	Nb-O3	1.999
Nb-O4	1.999	Nb-O4	1.977
Nb-O5	2.066	Nb-O5	2.033
Nb-O6	2.162	Nb-O6	1.985
Nb-O7	2.086	Nb-O7	2.040
Nb-O8	2.011	Nb-O19	2.138
Nb-N10	2.370	Nb-O20	2.831
O2-O3	1.526	O2-O3	1.527
O4-O8	1.533	O5-O6	1.530
O5-O7	1.530	O4-O7	1.532
C12-C15	1.537	C18-C11	1.521
C9-O6	1.307		
\angle O2-Nb-O3	43.9	\angle O2-Nb-O3	44.3
\angle O4-Nb-O8	44.9	\angle O4-Nb-O7	44.8
\angle O5-Nb-O7	44.2	\angle O5-Nb-O6	44.7
\angle O6-Nb-N10	72.1	\angle O3-Nb-O19	82.9

^aSee Fig. 5 for atomic numbering.

and experimental spectral data are anticipated as the calculated spectral data are obtained for those of the gas phase optimized geometries. These observed discrepancies appear to be acceptable as the average error for frequencies calculated with B3LYP functional was reported to be of the order 40-50 cm^{-1} for inorganic molecules.³⁷ Moreover, such deviations in the FTIR and Raman vibrational bands obtained from DFT based calculations on eight co-ordinated peroxo complexes of niobium(V) are not unprecedented.^{20f} Thus the results obtained from our theoretical calculations truly support our experimental findings and completely validate the predicted geometries for the synthesized complexes.

2.2 Catalytic activity of the complexes, **NbA** and **NbN**

2.2.1 Oxidation of sulfides to sulfoxides

Catalytic performances of the title pNb complexes in oxidation of various organic sulfides using 30% aqueous H_2O_2 as terminal oxidant in neat water, has been investigated. In a preliminary experiment, the reaction of MPS with H_2O_2 (1 equivalent) in presence of the water soluble catalyst, **NbA**, maintaining the catalyst: substrate molar ratio at 1 : 1000 was conducted in water at ambient temperature under magnetic stirring. The reaction proceeded rapidly within a reasonably short period of time in presence of each of the catalysts. The reaction under these conditions was however, observed to be mildly exothermic leading to the formation of a mixture of **1a** and **1b** in the molar ratio of 85:15, as presented in Table 6 (entry 1). Subsequently, the reaction conditions for selective sulfoxidation including substrate: oxidant stoichiometry, catalyst concentration, solvent type and reaction temperature were optimized using MPS as model substrate and the complex **NbA** as the catalyst. We have attempted to control the degree of oxidation by lowering the reaction temperature to 0 °C by conducting the reaction in an ice-bath.

Table 6 Optimization of reaction conditions for selective oxidation of methyl phenyl sulfide (MPS) by 30% H₂O₂ catalyzed by pNb complexes^a

Entry	Molar ratio Cat:MPS	30% H ₂ O ₂ (equiv.)	Solvent	Time (min)	Isolated Yield (%)	1a : 1b	TON	TOF (h ⁻¹)
1	1:1000 ^b	1	H ₂ O	75	76	85:15	760	608
2	1:1000 ^c	1	H ₂ O	75	70	100:0	700	560
3	1:500 ^c	2	H ₂ O	38	97	85:15	485	766
4	1:1000 ^c	2	H ₂ O	40	95	100:0	950	1425
5	1:2000 ^c	2	H ₂ O	43	96	100:0	1920	2679
6	1:2500^c	2	H₂O	50	97	100:0	2425	2910
7	1:3000 ^c	2	H ₂ O	75	95	100:0	2844	2275
8	1:2500 ^b	2	CH ₃ OH	115	75	100:0	1875	978
9	1:2500 ^b	2	CH ₃ CN	120	70	100:0	1750	875
10 ^d	1:2500 ^c	2	H ₂ O	95	97	55:45	2425	1531
11 ^e	1:2500 ^c	2	H ₂ O	20	96	100:0	2400	7200
12 ^f	-	2	H ₂ O	50	9	90:10	-	-

^aReactions were carried out with 5 mmol of substrate in 5 mL of solvent. Catalyst amount = 2.22 mg for 0.005 mmol of **NbA**. ^bReaction at room temperature. ^cReaction at 0 °C in ice bath. ^dNa₃[Nb(O₂)₄].13H₂O as catalyst, ^eUsing H₂SO₄ (1 mmol), ^fBlank experiment (without catalyst).

As has been anticipated, the reaction indeed proceeded smoothly to yield sulfoxide with 100% selectivity and nearly 70% conversion under these conditions. Complete oxidation of MPS to pure sulfoxide could be attained with excellent TOF (without affecting the selectivity) by increasing the oxidant: substrate molar ratio to 2 : 1, without altering the other reaction conditions.

Next, we have examined the effect of the catalyst amount on the rate and selectivity of the reaction under otherwise identical reaction conditions. As illustrated in Table 6, although at higher catalyst concentration the rate was faster and a reasonably good TOF could be attained even at catalyst : substrate ratio of 1 : 3000, the optimal catalyst : substrate molar ratio was however found to be 1 : 2500 for achieving highest TOF along with complete selectivity. The pNb species has an important contribution in facilitating the reactions was confirmed by conducting a control experiment without the catalyst. The reaction was extremely slow and non-selective in absence of the catalyst, affording a mixture of sulfoxide and sulfone in < 9 % yield under the optimized reaction condition (Table 6, entry 12). We have also compared the catalytic efficiency of the newly developed catalysts with neat tetraperoxoniobate (TPNB) complex Na₃[Nb(O₂)₄].13H₂O under analogous reaction conditions. As shown in Table 6 (entry 10), the reaction proceeded smoothly in presence of TPNB as well, although product selectivity could not be obtained under the maintained reaction condition. From these observations it is apparent that the co-ligand environment influences the catalytic activity of the pNb compounds.

In addition to water, we have screened the sulfoxidation reaction in relatively safer organic solvents such as CH₃OH and CH₃CN. The solvent effect has been evaluated in the oxidation of MPS. Interestingly, the catalytic protocol for sulfoxidation was found to be compatible with these organic solvents as well, however, the efficiency of the catalysts was observed to vary with the nature of the solvent. Although the catalysts are insoluble in neat organic solvents, including methanol or acetonitrile, in presence of aqueous H₂O₂ used as oxidant, each of the catalysts

dissolves completely in these water miscible solvents leading to the homogeneity of the catalytic process. Pertinent here is to mention that, we have strategically avoided the use of hazardous chlorinated solvents in the present work. The data presented in Table 6 (entries 8, 9) demonstrate that although the **NbA** is highly potent in methanol as well as in acetonitrile, MeOH proved to be relatively better solvent affording both product selectivity and high yield at ambient temperature (Table 6, entry 8). Significantly, the selective sulfoxidation in the chosen organic solvents could be achieved at room temperature. It is thus remarkable that by using the same set of catalyst it is possible to achieve selective oxidation of sulfide in water as well as in organic solvents under mild reaction conditions. Water however proved to be the best solvent with respect to catalyst efficiency as demonstrated by higher TOF and product selectivity, notwithstanding the insolubility of most of the chosen organic substrates in water. This is not surprising, keeping in view the observations made by Sharpless *et al.*,^{12b} that several reactions involving water insoluble organic reactants could proceed optimally in pure water. Our results are also in agreement with earlier findings that chemoselective sulfoxidation is favoured in polar protic solvent with high hydrogen bonding ability.³⁸

The sulfoxidation reaction has been carried out at the natural pH attained by the reaction mixture (*ca.* 5). However, a substantial increase in TOF was noted on addition of acid to the reaction medium (Table 6, entry 11). The finding is in accord with the reports related to other peroxo metal systems (Ti, Mo and W),³⁹ where it has been demonstrated that use of acidic additives led to an improvement in catalytic activity of the peroxometallates. The role of protons in the activation of titanium peroxo complexes has been extensively investigated by Kholdeeva and co-workers.^{39b} In the present work however, since our goal has been to maintain a mild reaction condition, addition of acid or other additives were avoided as far as possible. Therefore no attempt has been made to adjust the pH of the reaction.

Table 7 Selective oxidation of sulfides to sulfoxides catalysed by **NbA** and **NbN**^a

Entry	Substrate	NbA				NbN			
		Time (min)	Isolated Yield of sulfoxide (%)	TON ^b	TOF ^c (h ⁻¹)	Time (min)	Isolated yield of sulfoxide (%)	TON ^b	TOF ^c (h ⁻¹)
1.		50	97	2425	2910	45	96	2400	3200
		50	93 ^d	2325	2790	45	94 ^d	2350	3133
		50	96 ^e	2400	2880	45	95 ^e	2375	3166
2.		45	97	2425	3233	40	95	2375	3562
3.		85	93	2325	1641	75	94	2350	1880
4.		240	95	2375	593	225	93	2325	620
5.		115	97	2425	1265	105	95	2375	1357
6.		55	96	2400	2618	50	95	2375	2850
7.		210	93	2325	664	195	94	2350	723
8.		30	97	2425	4850	25	96	2400	5760
9.		40	96	2400	3600	35	93	2325	3985
10.		40	97	2425	3637	35	95	2375	4071

^aOptimized condition: 5 mmol substrate, 10 mmol 30% H₂O₂ and 0.002 mmol catalyst in H₂O at 0 °C. ^bTON (turnover number) = mmol of product per mmol of catalyst. ^cTOF (turnover frequency) = mmol of product per mmol of catalyst per hour. ^dYield of 6th reaction cycle, ^eScale up data (6.24g of MPS).

155

The afore mentioned findings were further exploited to obtain pure sulfoxide from series of aryl alkyl, aryl vinyl, aryl alcohol and dialkyl sulfides listed in Table 7. Evidently, both the catalysts were effective in leading to the facile and selective transformation of each of the substrates to the corresponding sulfoxide in impressive yield, although, catalyst **NbN** displayed relatively superior activity. The transformations worked well for both aliphatic as well as aromatic substrates irrespective of having electron donating or electron withdrawing moieties. The nature of the substrate and attached substituent however, appeared to influence the rates of oxidation.^{8g,11b} The observed trend in variations in the rate of oxidation of the chosen substrates is consistent with the previous findings that with increasing nucleophilicity of the sulfide rate of oxidation by H₂O₂ increases.^{8g,11b} It is therefore not unexpected that dialkyl sulfides were oxidized by H₂O₂ at a faster rate leading to the highest TOF, relative to conjugated systems such as allylic and vinylic sulfides or aromatic sulfides. It is notable that even in the case of a less nucleophilic diaromatic sulfide the corresponding sulfoxide was effectively obtained.

A salient feature of the methodology, which enhances the synthetic utility of the oxidations, is the excellent chemoselectivity displayed by the catalysts for sulfur group of substituted sulfides such as allylic, vinylic and alcoholic sulfides, with co-existing sensitive functional groups (Table 7, entries 3-5). Importantly, allylic and vinylic sulfoxides were obtained without epoxidation product. Moreover, -OH group of alcoholic sulfides and benzylic C-H bond remained unaffected when the benzylic and alcoholic sulfides could be oxidized to corresponding sulfoxide under the maintained reaction conditions. Potential of the developed protocol for scaled-up synthetic application has been demonstrated by conducting the oxidation with 6.24 g of thioanisole (ten-fold scale) under optimized condition (Table 7, entry 1^e). The H₂O₂ efficiency in the oxidations in presence of both the catalysts **NbA** and **NbN** was found to be higher than 90%. The H₂O₂ efficiency which is a measure of the effective use of H₂O₂, has been defined as (100 × mole of H₂O₂ consumed in the formation of oxyfunctionalized products/mole of H₂O₂ converted)^{11a} [Text S4, (ESI†)].

Table 8 Optimization of reaction conditions for **NbA** catalyzed selective oxidation of methyl phenyl sulfide (MPS) to sulfone^a

Entry	Molar ratio (Catalyst:MPS)	H ₂ O ₂ (equiv.)	Solvent	Time (min)	Isolated yield (%)	1a:1b	TON	TOF(h ⁻¹)
1.	1:1000	2	H₂O	80	96	0:100	960	720
2.	1:2000	2	H ₂ O	175	95	0:100	1900	651
3.	1:2500	2	H ₂ O	240	96	25:75	2400	600
4.	1:1000	2	CH ₃ OH	240	96	70:30	960	240
5.	1:1000	2	CH ₃ CN	240	93	75:25	930	232

^aReactions are carried out with 5 mmol of substrate in 5 mL of solvent at room temperature.

2.2.2 Oxidation of sulfides to sulfones

Clean conversion of MPS to sulfone could be achieved with high yield in aqueous medium, in presence of each of the catalysts, simply by extending the reaction time after initial formation of sulfoxides and conducting the reaction at room temperature. The optimization of reaction conditions, accomplished by using MPS as substrate and **NbA** as catalyst, revealed that the best rate and TOF could be obtained by

maintaining the catalyst: substrate ratio at 1:1000, using 2 equivalents of H₂O₂ (Table 8, entry 1).

Apart from MPS, the protocol could be conveniently applied to obtain pure sulfone from a variety of aromatic and aliphatic sulfides as shown in Table 9. The transformations were chemoselective (Table 9, entries 3, 4, 5.) and amenable for scale-up (Table 9, entry 1^e) as has been observed in case of sulfoxidation reaction. These findings underscore the synthetic value of the methodology.

Table 9 Selective oxidation of sulfides to sulfones catalyzed by **NbA** and **NbN**^a

Entry	Substrate	NbA				NbN			
		Time (min)	Isolated yield of sulfone (%)	TON ^b	TOF ^c (h ⁻¹)	Time (min)	Isolated yield of sulfone (%)	TON ^b	TOF ^c (h ⁻¹)
1.		80	96	960	720	70	97	970	831
		80	93 ^d	930	697	70	93	930	797
		80	95 ^e	950	712	70	94 ^e	940	805
2.		75	95	950	760	65	97	970	895
3.		145	93	930	384	135	94	940	431
4.		255	94	940	221	250	93	930	235
5.		190	97	970	306	180	95	950	316
6.		90	95	950	633	80	94	940	705
7.		315	93	930	177	310	93	930	180
8.		65	94	940	867	55	96	960	1047
9.		70	93	930	797	60	93	930	930
10.		70	95	950	814	60	94	940	940

^aOptimized condition: 5 mmol substrate, 10 mmol 30% H₂O₂ and 0.005 mmol catalyst in H₂O at RT. ^bTON (turnover number) = mmol of product per mmol of catalyst. ^cTOF (turnover frequency) = mmol of product per mmol of catalyst per hour. ^dYield of 6th reaction cycle. ^eScale up data (6.24g of MPS).

2.2.3 Recyclability of the catalysts

The reusability of the catalysts for subsequent cycles of oxidation was assessed by employing MPS as the substrate. The catalysts afforded regeneration *in situ* after separation of the organic product from the reaction mixture on completion of the reaction and could be reused without further conditioning. Regeneration was accomplished simply by charging the aqueous part of the spent reaction mixture with 30% H₂O₂ and fresh lot of substrate, on completion of each reaction cycle. In an alternative approach the regenerated catalysts could also be isolated into solid state by solvent induced precipitation with acetone after treating the aqueous extract of the spent reaction mixture with 30% H₂O₂. Nevertheless, the *in-situ* regeneration of the catalyst offers obvious advantages as the procedure does not require tedious separation and subsequent purification steps, which are usually associated with soluble catalysts.^{12a} The activity and selectivity of the catalysts remained unaltered at least up to 6 reaction cycles as illustrated in Table 7 (entry 1^d), Table 9 (entry 1^d) and Fig S6 (ESI†). In order to further confirm that the catalysts remain intact after their use in catalytic cycles, the recovered catalysts were characterized by elemental analysis and spectral studies. The IR and Raman spectra of each of the regenerated catalysts resembled closely the corresponding spectrum of the starting catalyst, displaying the typical absorptions for triperoxoniobium moiety and respective metal bound co-ligand indicating that the coordination environment of the complexes was not altered during the catalytic process. The IR spectrum of the regenerated catalyst **NbA** is presented in Fig. S1 (c) (ESI†). No significant change was observed in the niobium and peroxide content of the recovered catalysts in comparison to the respective original complex. It is thus evident that the metal complexes retain their structural integrity even after several catalytic cycles.

Interestingly, the procedure with **NbA** used as catalyst, provided an overall TOF of approximately *ca.* 17,130 h⁻¹ (*ca.* 18,999 h⁻¹ for **NbN**) after 6 cycles of oxidation of MPS to sulfoxide and *ca.* 4,259 h⁻¹ (*ca.* 4,884 h⁻¹ with **NbN**) for conversion to sulfone. The results further demonstrate the superior activity of the catalysts under mild condition, over other reported methods for sulfide oxidation involving Nb(V) catalysts,^{20a-f} as well as many other protocols based on Mo(VI) or W(VI) / H₂O₂^{7b-e,8b-e,g,10c,g,h,38a,40} systems including the polymer supported heterogeneous Mo(VI) catalysts reported recently by

us^{7b}.

2.2.4 The proposed mechanism

Based on our results and taking into account our earlier findings on catalytic activity of some other peroxometal systems,^{7b,8a} a credible mechanism for the pNb catalyzed selective oxidation of sulfides to sulfoxides or sulfone by H₂O₂ has been proposed (Fig. 6), which satisfactorily describes the principal features of our findings from the present study.

As shown in Fig. 6, with catalyst **NbA** as a representative, it is possible that the reaction proceeds through the formation of a diperoxonioate intermediate **II**, subsequent to facile transfer of electrophilic oxygen from the triperoxoniobium complex **I** to the substrate **V** to yield sulfoxide (reaction a). The intermediate **II** combines with peroxide of H₂O₂ to regenerate the starting triperoxoniobate complex (reaction b) leading to a catalytic cycle. The resulting sulfoxide formed may undergo further oxidation in a separate cycle by reacting with a triperoxo Nb species, to yield sulfone (reaction c). The sulfone formation thus seems to be a two step process. The greater ease of oxidation of sulfide to sulfoxide compared to the second oxidation of sulfoxide to sulfone is likely to be a consequence of higher nucleophilicity of sulfide relative to sulfoxide. The proposed mechanism is in line with the reaction pathway proposed previously for peroxoniobate catalysed oxidation of sulfide.^{18a,d,20g}

It is worthy to note that, although the mechanism of action of peroxo complexes of other d⁰ metals such V(V), Mo(VI) and W(VI) has been extensively investigated in organic oxidations, chemistry of Nb(V) peroxide still remains relatively unexplored.^{7b,d,8a,16e,21d,24,40a,d,41} The previous work from several laboratories including ours,^{7b,8a,16e,f} have shown that during substrate oxidation performed by active diperoxo complexes of Mo(VI) or W(VI) a more stable monoperoxo species is formed which is practically inactive in oxidation.^{7d,24,41k-n} Taking into account this finding, it is reasonable to expect the formation of a less reactive diperoxonioate (**DPNb**) intermediate, from an active triperoxoniobate (**TPNb**) species during sulfide oxidation, as shown in the proposed mechanism (reaction intermediate, **II**). In order to establish the involvement of such an intermediate in the reaction pathway a separate experiment was conducted using **NbA** as stoichiometric oxidant of MPS, maintaining the **NbA** : substrate molar ratio at 1:1, in absence of H₂O₂ at 0 °C. The substrate was completely and selectively transformed into sulfoxide within a reaction time of *ca.* 40 minutes. The product

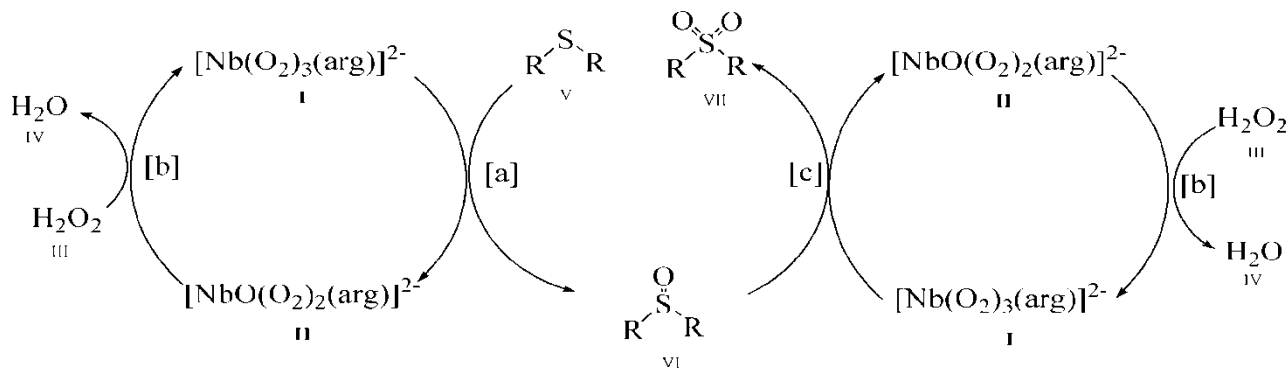


Fig. 6 The proposed mechanism.

isolated from the aqueous part of the spent reaction mixture was subsequently subjected to spectral and elemental analysis. The data obtained indicated a 1:2 ratio for Nb: peroxy suggesting clearly the formation of a **DPNb** species. This was further confirmed from the IR spectrum which showed, in addition to the co-ordinated amino acid ligands, two distinct bands characteristic of a **DPNb** moiety [Fig S1 (d) (ESI†)], in contrast to the three peroxy absorptions of the original triperoxoniobium catalyst. Similar reaction of MPS conducted with the isolated **DPNb** complex was noted to be extremely slow, as has been anticipated, remaining incomplete even after 14 h of reaction time. The aforementioned findings lent further credence to the proposed mechanism.

3. Experimental Section

3.1 Materials

Acetone, hydrogen peroxide, acetonitrile, methanol, ethylacetate, petroleum ether, diethyl ether, silica gel (60-120 mesh), (RANKEM), L-Arginine (CDH, New Delhi, India), Nicotinic acid (HIMEDIA) sodium hydroxide, sodium sulfate (E. Merck, India). Niobium pentoxide, methyl phenyl sulfide (MPS), methyl p-tolyl sulfide (MpTS), ethyl phenyl sulfide (EPS), dimethyl sulfide (DMS), dibutyl sulfide (DBS), phenylvinyl sulfide (PVS), 2-(phenylthio)ethanol (PTE), dihexyl sulfide (DHS), diphenyl sulfide (DPS) and allyl phenyl sulfide (APS) were obtained from Sigma–Aldrich Chemical Company, Milwaukee, USA. The water used for solution preparation was deionized and distilled.

3.2 Synthesis of the complexes

3.2.1 Preparation of sodium tetraperoxoniate¹⁸¹

Sodium tetraperoxoniate, $\text{Na}_3[\text{Nb}(\text{O}_2)_4] \cdot 13\text{H}_2\text{O}$ was prepared by the reported method.¹⁸¹ In a nickel crucible, 1 g of Nb_2O_5 and 1.85 g of NaOH were fused together at 700 °C. The solid obtained was cooled and dissolved in 100 ml of 1 M aqueous H_2O_2 . Unreacted Nb_2O_5 was filtered off and the filtrate was allowed to settle at 5 °C for 24 h to afford white crystalline $\text{Na}_3[\text{Nb}(\text{O}_2)_4] \cdot 13\text{H}_2\text{O}$.

3.2.2 Synthesis of peroxoniobate complex, $\text{Na}_2[\text{Nb}(\text{O}_2)_3(\text{arg})] \cdot 2\text{H}_2\text{O}$ (NbA)

Solid $\text{Na}_3[\text{Nb}(\text{O}_2)_4] \cdot 13\text{H}_2\text{O}$ (0.6550g, 1.25 mmol) was dissolved in 30% H_2O_2 (4 ml, 25 mmol) in a 250 ml beaker in an ice-bath. To this solution, L-arginine was added gradually with constant stirring, maintaining the temperature below 4 °C. At this stage pH of the solution was recorded to be ca. 8. Dilute HNO_3 solution (4M) was added dropwise to the solution with continuous stirring until the pH was lowered to 6. The resulting solution was allowed to stand for 3 h in an ice bath. A white pasty mass separated out on adding pre-cooled acetone to this mixture under vigorous stirring. The supernatant liquid was decanted off and the residue was treated repeatedly with acetone under scratching. The microcrystalline product obtained was separated by centrifugation and dried *in vacuo* over concentrated sulfuric acid.

3.2.3 Synthesis of peroxoniobate complex, $\text{Na}_2[\text{Nb}(\text{O}_2)_3(\text{nic}(\text{H}_2\text{O}))] \cdot \text{H}_2\text{O}$ (NbN):

The procedure consisted of gradual addition of nicotinic acid (1.25 mmol) with constant stirring to a solution of $\text{Na}_3[\text{Nb}(\text{O}_2)_4] \cdot 13\text{H}_2\text{O}$ (0.6550g, 1.25 mmol) in 30 % H_2O_2 (4 ml, 25 mmol) in an ice-bath. The pH 3 of the reaction solution at this stage was raised to ca. 6 by drop wise addition of NaOH solution (8M) with stirring. After allowing the solution to stand for 3 h, pre-cooled acetone was added to it under continuous stirring. The white colour pasty mass obtained from the solution after decanting the supernatant liquid, was treated repeatedly with acetone to isolate the product as white microcrystalline solid. The product obtained was separated by centrifugation and dried *in vacuo* over concentrated sulfuric acid.

3.3 Elemental Analysis

The elemental analyzer Perkin-Elmer 2400 series II was used for C, H and N elemental analysis of the synthesized compounds. Niobium content was estimated gravimetrically as $\text{NbO}(\text{C}_{13}\text{H}_{10}\text{NO}_2)_3$ ⁴² and with the atomic absorption spectroscopy (AAS). Niobium, sodium, C and N composition contents were also obtained from EDX analysis. In addition, sodium content was quantified with ionometer (ORION VERSASTER). Peroxide content for the compounds was determined by adding a weighed amount of the compound to a cold solution of 1.5% boric acid (W/V) in 0.7 M sulfuric acid (100 mL) and titration with standard sodium thiosulfate solution.⁴³

3.4 Physical and Spectroscopic measurements

The IR spectra were recorded at ambient temperature by making pressed pellets of the compounds with KBr pellets in a Perkin-Elmer spectrum 100 FTIR spectrophotometer. Raman spectra of the compounds were recorded by Renishaw InVia Raman microscope that was equipped with an argon ion laser with an excitation wavelength of 514 nm and laser maximum output power of 20 mW. The measurement parameters were 10 s exposure time, 1 accumulation, laser power 10% of output power and 50× objective and the spectral resolution was set to 0.3 cm^{-1} . Thermogravimetric analysis was performed in SHIMADZU TGA-50 system at a heating rate of 10 °C min^{-1} under an atmosphere of nitrogen using an aluminium pan. Energy-dispersive X-ray analysis was done by using JEOL JSM-6390LV Scanning Electron Micrograph attached with an energy-dispersive X-ray detector. Atomic Absorption Spectrometry was done in Thermo iCE 3000 series Atomic absorption spectrophotometer model analyst 200. The ¹³C NMR spectra for Arginine, NbA, Nicotinic acid and NbN were recorded using a JEOL JNM-ECS400 spectrometer at a carbon frequency of 100.5 MHz, 4096 X-resolution points, number of scans 1000-20000, 1s of acquisition time, 30° pulse length (D_2O as solvent). ¹H NMR study for the synthesised complexes along with free ligands has been carried out with JEOL JNM-ECS400 spectrometer with 16 scans, 2 s of acquisition time and 45° pulse length (D_2O as solvent). The ¹H and ¹³C NMR spectra of organic sulfoxides and sulfones were recorded in a JEOL JNM-ECS400 spectrometer (CDCl_3 as solvent and TMS as an internal standard). Melting points were determined in open capillary tubes on Büchi Melting

Point B-540 apparatus and are uncorrected. GC analysis was carried out on a CIC, Gas Chromatograph model 2010 using a SE-52 packed column (length 2 m, 1/8" OD) with a Flame Ionization Detector (FID), and nitrogen as the carrier gas (30 mL min⁻¹).

3.5 Catalytic Activity

3.5.1 General procedure for oxidation of sulfides to sulfoxides (Catalyst: NbA, NbN) at 0 °C

In a representative procedure, organic substrate (5 mmol) was added to a solution of catalyst (0.002 mmol) in water (5 mL) and then oxidant 30% H₂O₂ (1.13 mL, 10 mmol) was added, maintaining molar ratio of catalyst : substrate at 1 : 2500 and substrate : H₂O₂ at 1 : 2, in a 50 mL round-bottomed flask. The reaction was conducted at 0 °C in an ice bath under continuous stirring. The progress of the reaction was monitored by thin layer chromatography (TLC). After completion of the reaction, the products were extracted with diethyl ether and dried over anhydrous Na₂SO₄ and distilled under reduced pressure to remove excess diethyl ether. The corresponding sulfoxide obtained was purified by column chromatography on silica gel using ethyl acetate and n-hexane (1:9).

The products obtained were characterized by IR, ¹H NMR, ¹³C NMR spectroscopy and in case of solid sulfoxide products, in addition to the above spectral analysis, we have also carried out melting point determination (see Supporting Information).

3.5.2 General procedure for oxidation of sulfides to sulfones (Catalyst: NbA, NbN) at room temperature

To stirred solution of catalyst (0.005 mmol) and 30 % H₂O₂ (10 mmol), the organic substrate (5 mmol) was added in water (5 mL) maintaining molar ratio of catalyst: substrate at 1: 1000 and substrate: H₂O₂ at 1: 2 at room temperature (RT) under continuous stirring. The reaction was monitored by thin layer chromatography (TLC). After completion of the reaction, the products were extracted with diethyl ether and dried over anhydrous Na₂SO₄ and distilled under reduced pressure to remove excess diethyl ether. The corresponding sulfone obtained was purified by column chromatography on silica gel using ethyl acetate and n-hexane (1:9).

The IR, ¹H NMR, ¹³C NMR spectroscopy tools were used to characterize the products. In addition to the above spectral analysis, we have also carried out melting point determination for the products (see Supporting Information).

3.6 Regeneration of the catalyst

Any of the following procedures could be adopted to regenerate the catalysts for reuse. The regeneration of the catalyst was carried out for the reaction using methyl phenyl sulfide (MPS). After completion of the oxidation reaction and subsequent extraction of the organic reaction product, the aqueous part of the reaction mixture was transferred to a 250 mL beaker. Keeping the solution in an ice bath, 30% H₂O₂ was added to it maintaining the Nb : peroxide ratio 1 : 2, followed by addition of pre-cooled acetone with constant stirring until a white pasty mass separated out. From this precipitate the catalyst was finally obtained as microcrystalline solid by following the work-up procedure mentioned under Section 3.2.2. The regenerated pNb catalyst was then placed into a fresh reaction mixture

consisting of MPS, hydrogen peroxide in water, and the reaction was allowed to proceed under optimised condition as mentioned under Section 3.5.1 (for sulfoxide) or Section 3.5.2 (for sulfone).

The progress of the reaction was monitored by thin layer chromatography (TLC). After completion of the reaction, the process is repeated for a total of six reaction cycles.

In an alternative procedure, recycling of the catalyst could be performed *in situ*, after completion of the reaction cycle and extraction of the organic reaction product. Regeneration of the used reagent could be achieved by adding 30% H₂O₂ and fresh lot of substrate to the aqueous portion of the spent reaction mixture, maintaining the same recipe as mentioned under Sections 3.5.1 (for sulfoxide) or Section 3.5.2 (for sulfone), and conducting the reaction under optimised condition. Each of the procedures was repeated for six reaction cycles.

3.7 Computational Details

The density functional theory (DFT)³⁶ calculations were performed using Gaussian09 programme⁴⁴ at B3LYP/LANL2DZ level of theory. The ground state geometry of the two niobium complexes were obtained in gas phase and the minima of the optimized structures were verified by the absence of imaginary frequencies.

Conclusions

In summary, a pair of new heteroligand triperoxoniobium (V) complexes have been synthesized, characterized and successfully applied in the selective oxidation of variously substituted sulfides to selectively obtain sulfoxide or sulfone with 30% H₂O₂ in neat water. The reactions proceed under mild condition to afford the resulting products with impressive yield and TON or TOF. The catalysts display excellent chemoselectivity toward sulfur group of substrates with other oxidizable functional groups, including hydroxyl group and C=C bonds. The adherence of the developed protocol to the principles of green chemistry is assured by the fact that the reactions employ, apart from neat water as a standard green solvent and aqueous 30% H₂O₂ as oxidant, a non-toxic pNb catalyst which can be reused in subsequent cycles without losing its activity. In addition, the oxidations are absolutely free from organic co-solvent, co-catalyst or any other auxiliaries, involve easy work-up procedure and is amenable for ready scalability. All these features make the catalytic strategies presented attractive and interesting from both economic and environmental perspectives.

Acknowledgements

The authors gratefully acknowledge the Department of Science and Technology, New Delhi, India, for providing financial support. We are also grateful to University Grants Commission, Basic Science Research Fellowship, New Delhi, India for providing Junior Research Fellowship to S.R.G. We thank Dr. B. Choudhury, Department of Physics, Tezpur University, Tezpur, Assam, India for Raman spectra.

Notes and references

- ³⁴⁵ ^a Department of Chemical Sciences, Tezpur University, Napaam, Tezpur - 784 028, Assam, India. Tel: +91-3712-267007, +91-9435380222(Off); E-mail: nsi@tezu.ernet.in, nashreen.islam@rediffmail.com
- † Electronic Supplementary Information (ESI) available: FTIR, ¹³C and ¹H NMR spectra of complexes, hydrogen peroxide efficiency, characterization of sulfoxides and sulfones, bar diagram for recyclability of catalyst. See DOI: 10.1039/b000000x/
- (a) H. L. Holland, *Chem. Rev.*, 1988, **88**, 473-485; (b) M. Tanaka, H. Yamazaki, H. Hokusui, N. Nakamichi and H. Sekino, *Chirality*, 1997, **9**, 17-21; (c) H. Cotton, T. Elebring, M. Larsson, L. Li, H. H. Sorensen and S. Von Unge, *Tetrahedron: Asymmetry*, 2000, **11**, 3819-3825; (d) M. C. Carreno, *Chem. Rev.*, 1995, **95**, 1717-1760; (e) S. Patai and Z. Rappoport, *Synthesis of Sulfoxides, Sulfoxides and Cyclic Sulfides*, J. Wiley, Chichester, 1994.
 - (a) I. Fernandez and N. Khair, *Chem. Rev.*, 2003, **103**, 3651-3706; (b) J. Legros, J. R. Dehli and C. Bolm, *Adv. Synth. Catal.*, 2005, **347**, 19-31.
 - (a) V. Hulea, F. Fajula and J. Bousquet, *J. Catal.*, 2001, **198**, 179-186; (b) M. Iwamoto, Y. Tanaka, J. Hirosumi, N. Kita and S. Triwahyono, *Micropor. Mesopor. Mater.*, 2001, **48**, 271-277.
 - (a) S. Hussain, D. Talukdar, S. K. Bharadwaj, M. K. Chaudhuri, *Tetrahedron Lett.*, 2012, **53**, 6512-6515; (b) V. Conte and B. Floris, *Dalton Trans.*, 2011, **40**, 1419-1436; (c) V. Conte, F. Fabbianesi, B. Floris, P. Galloni, D. Sordi, I.C.W.E. Arends, M. Bonchio, D. Rehder and D. Bogdal, *Pure Appl. Chem.*, 2009, **81**, 1265-1277; (d) F. Gregori, I. Nobili, F. Bigi, F. Maggi and G. Predieri, *J. Mol. Catal. A: Chem.*, 2008, **286**, 124-127; (e) F. Di Furia, G. Modena, R. Curci, *Tetrahedron Lett.*, 1976, **17**, 4637-4638.
 - (a) L. Xu, J. Cheng and M. L. Trudell, *J. Org. Chem.* 2003, **68**, 5388-5391; (b) N. S. Venkataramanan, G. Kuppuraj and S. Rajagopal, *Coord. Chem. Rev.*, 2005, **249**, 1249-1268.
 - (a) F. Rajabi, S. Naserian, A. Primo and R. Luque, *Adv. Synth. Catal.*, 2011, **353**, 2060-2066. (b) H. Egami and T. Katsuki, *J. Am. Chem. Soc.*, 2007, **129**, 8940-8941.
 - (a) R. D. Chakravarthy, V. Ramkumar and D. K. Chand, *Green Chem.*, 2014, **16**, 2190-2196; (b) J. J. Boruah, S. P. Das, S. R. Ankireddy, S. R. Gogoi and N. S. Islam, *Green Chem.*, 2013, **15**, 2944-2959; (c) K. Kaczorowska, Z. Kolarska, K. Mitka and P. Kowalski, *Tetrahedron*, 2005, **61**, 8315-8327; (d) N. Gharah, S. Chakraborty, A. K. Mukherjee and R. Bhattacharyya, *Inorg. Chim. Acta*, 2009, **362**, 1089-1100; (e) N. M. Gresley, W. P. Griffith, A. C. Laemmel, H. I. S. Nogueira and B. C. Parkin, *J. Mol. Catal. A: Chem.*, 1997, **117**, 185-198.
 - (a) S. P. Das, J. J. Boruah, N. Sharma and N. S. Islam, *J. Mol. Catal. A: Chem.*, 2012, **356**, 36-45. (b) B. Karimi, M. Ghoreishi-Nezhad and J. H. Clark, *Org. Lett.*, 2005, **7**, 625-628; (c) X.-Y. Shi, J.F. Wei, *J. Mol. Catal. A: Chem.*, 2008, **280**, 142-147; (d) D.H. Koo, M. Kim, S. Chang, *Org. Lett.*, 2005, **7**, 5015-5018; (e) Y.M.A. Yamada, H. Tabata, M. Ichinohe and H.T.S. Ikegami, *Tetrahedron*, 2004, **60**, 4087-4096; (f) B. M. Choudary, B. Bharathi, C. V. Reddy and M. L. Kantam, *J. Chem. Soc. Perkin Trans.*, 2002, **1**, 2069-2074; (g) K. Sato, M. Hyodo, M. Aoki, X.-Q. Zheng and R. Noyori, *Tetrahedron*, 2001, **57**, 2469-2476.
 - K.J. Stanger, J.W. Wiench, M. Pruski, J.H. Espenson, G.A. Kraus and R.J. Angelici, *J. Mol. Catal. A: Chem.*, 2006, 243, 158-169.
 - (a) P. S. Kulkarni and C. A. M. Afonso, *Green Chem.*, 2010, **12**, 1139-1149; (b) M. V. Gómez, R. Caballero, E. Vázquez, A. Moreno, A. Hoz and Á. Díaz-Ortiz, *Green Chem.*, 2007, **9**, 331-336; (c) R. Noyori, M. Aoki and K. Sato, *Chem. Commun.*, 2003, 1977-1986; (d) K. Sato, M. Aoki and R. Noyori, *Science*, 1998, **281**, 1646-1647; (e) C. W. Jones, *Applications of Hydrogen Peroxide and Derivatives*; Royal Society of Chemistry: Cambridge, 1999. (f) *In Catalytic Oxidations with Hydrogen Peroxide as Oxidant*, ed. G. Strukul, Kluwer Academic Publishers: Dordrecht, 1992; (g) P. Kowalski, K. Mitka, K. Ossowska and Z. Kolarska, *Tetrahedron*, 2005, **61**, 1933-1953; (h) B. M. Choudary, B. Bharathi, C. V. Reddy and M. L. Kantam, *J. Chem. Soc., Perkin Trans. 1*, 2002, 2069-2074. (i) G. Strukul and A. Scarso, *Environmentally Benign Oxidants, in Liquid Phase Oxidation via Heterogeneous Catalysis*, ed. M. G. Clerici and O. A. Kholdeeva, John Wiley & Sons, Inc., Hoboken, New Jersey, 2013, ch. 1, pp 1-20.
 - (a) V. Hulea, A.-L. Maciucă, F. Fajula and E. Dumitriu, *Appl. Catal. A*, 2006, **313**, 200-207; (b) B. S. Lane and K. Burgess, *Chem. Rev.*, 2003, **103**, 2457-2474.
 - (a) U. M. Lindstrom, *Chem. Rev.* 2002, **102**, 2751-2772 (b) S. Narayan, J. Muldoon, M. G. Finn, V. V. Fokin, H. C. Kolb and K. B. Sharpless, *Angew. Chem. Int. Ed.* 2005, **44**, 3275-3279.
 - (a) U. M. Lindstrom, *Organic Reactions in Water*; ed. Blackwell Publishing: Oxford, 2007; (b) D. C. Rideout and R. J. Breslow, *Am. Chem. Soc.* 1980, **102**, 7816-7817.
 - (a) K. Surendra, N. S. Krishnaveni, V. P. Kumar, R. Sridhar and K. R. Rao, *Tetrahedron Lett.*, 2005, **46**, 4581-4583; (b) K. L. Prasanth and H. Maheswaran, *J. Mol. Catal. A: Chemical*, 2007, **268**, 45-49; (c) X.-M. Zeng, J.-M. Chen, A. Yoshimura, K. Middletonb and V. V. Zhhdankin, *RSC Advances*, 2011, **1**, 973-977; (d) A. Rezaeifard, M. Jafarpour, A. Naeimi and M. Salimi, *Inorg. Chem. Commun.*, 2012, **15**, 230-234; (e) Y. Imada, T. Kitagawa, H.-K. Wanga, N. Komiya and T. Naota, *Tetrahedron Lett.*, 2013, **54**, 621-624; (f) B. Yu, C.-X. Guo, C.-L. Zhong, Z.-F. Diao and L.-N. He, *Tetrahedron Lett.*, 2014, **55**, 1818-1821.
 - J. J. Boruah, S. P. Das, R. Borah, S. R. Gogoi, N. S. Islam, *Polyhedron*, 2013, **52**, 246-254.
 - (a) D. Kalita, S. Sarmah, S. P. Das, D. Baishya, A. Patowary, S. Baruah and N. S. Islam, *React. Funct. Polym.*, 2008, **68**, 876-890; (b) S. Sarmah, D. Kaita, P. Hazarika, R. Borah and N. S. Islam, *Polyhedron*, 2004, **50**, 8046-8062; (c) S. Sarmah, P. Hazarika, R. Borah, N. S. Islam, A. V. S. Rao and T. Ramasarma, *Mol. Cell. Biochem.*, 2002, **236**, 95-105; (d) S. Sarmah and N. S. Islam, *J. Chem. Res.*, 2001, 172-174; (e) P. Hazarika, D. Kalita, S. Sarmah, R. Borah and N. S. Islam, *Polyhedron*, 2006, **25**, 3501-3508; (f) S. P. Das, J. J. Boruah, H. Chetry and N. S. Islam, *Tetrahedron Lett.*, 2012, **53**, 1163-1168.
 - K. Rydzynski and D. Pakulska, *Patty's Industrial Hygiene and Toxicology*, John Wiley & Sons Press, 2012.
 - (a) Hiromichi Egami, Takuya Oguma, and Tsutomu Katsuki, *J. Am. Chem. Soc.* 2010, **132**, 5886-5895; (b) H. Egami and T. Katsuki, *Angew. Chem. Int. Ed.*, 2008, **47**, 5171-5174; (c) M. Kirihara, J. Yamamoto, T. Noguchi, A. Itou, S. Naito, Y. Hirai, *Tetrahedron* 2009, **65**, 10477-10484; (d) D. Bayot, M. Devillers, *Coord. Chem. Rev.*, 2006, **250**, 2610-2626; (e) F. V. Tkhai, A. V. Tarakanova, O. V. Kostyuchenko, B. N. Tarasevich, N. S. Kulikov and A. V. Anisimov, *Theoretical Foundations of Chemical Engineering*, 2008, **42**, 636-642; (f) E. V. Rakhmanov, A. L. Maximov, A. V. Tarakanova, F. V. Tkhai and A. V. Anisimov, *Moscow University*

- 460 *Chemistry Bulletin*, 2010, **65**, 380–383. (g) E. V. Rakhmanov, Zhong Sinyan, A. V. Tarakanova, A. V. Anisimov, A. V. Akopyan and N. S. Baleeva, *Russ. J. Gen. Chem.*, 2012, **82**, 1118–1121; (h) 520 C. M. S. Batista, S. C. S. Melo, G. Gelbard and E. R. Lachter, *J. Chem. Res. (S)*, 1997, 92–93; (i) L. C. Passoni, M. R. H. Siddiqui, A. Steiner and I. V. Kozhevnikov, *J. Mol. Catal. A: Chemical*, 2000, 465 **153**, 103–108.
19. (a) V. Conte and F. Di Furia, in *Catalytic Oxidations with Hydrogen Peroxide as Oxidant*, ed. G. Strukul, Kluwer Academic Publishers, The Netherlands, 1992, p. 223. (b) V. Conte, F. Di Furia and S. Moro, *J. Mol. Catal.*, 1997, **120**, 93–99. (c) V. Conte, F. Di Furia and S. Moro, *J. Mol. Catal. A*, 1997, **117**, 139–149. (d) H. Mimoun, L. Saussine, E. Daire, M. Postel, J. Fischer and R. Weiss, *J. Am. Chem. Soc.*, 1983, **105**, 3101–3110.
20. (a) D. Bayot, B. Tinant, B. Mathieu, J.-P. Declercq and M. Devillers, *Eur. J. Inorg. Chem.*, 2003, 737–743; (b) D. Bayot, B. Tinant and M. Devillers, *Inorg. Chem.*, 2004, **43**, 5999–6005; (c) D. Bayot, M. Degand and Michel Devillers, *J. Solid State Chem.*, 2005, **178**, 2635–2642; (d) D. Bayot, B. Tinant and M. Devillers, *Inorg. Chem.*, 2005, **44**, 1554–1562; (e) D. Bayot, M. Degand, B. Tinant and M. Devillers, *Inorg. Chim. Acta*, 2006, **359**, 1390–1394; (f) A. Maniatakou, C. Makedonas, C. A. Mitsopoulou, C. Raptopoulou, I. Rizopoulou, A. Terzis and A. Karaliota, *Polyhedron*, 2008, **27**, 3398–3408; (g) A. Maniatakou, S. Karaliota, M. Mavri, C. Raptopoulou, A. Terzis and A. Karaliota, *J. Inorg. Biochem.*, 2009, 485 **103**, 859–868; (h) A. C. Dengel and W. P. Griffith, *Polyhedron*, 1989, **8**, 1371–1377; (i) Y. Narendar and G. L. Messing, *Chem. Mater.*, 1997, **9**, 580–587.
21. (a) C. Djordjevic, N. Vuletic, M. L. Renslo, B. C. Puryear and R. Alimard, *Mol. Cell Biochem.*, 1995, **153**, 25–29; (b) D. Kalita, R. C. Deka and N. S. Islam, *Inorg. Chem. Commun.*, 2007, **10**, 45–48; (c) P. Hazarika, S. Sarmah, D. Kalita and N. S. Islam, *Transition Met. Chem.*, 2008, **33**, 69–77; (d) D. Kalita, S. P. Das and N. S. Islam, *Biol. Trace Elem. Res.*, 2009, **128**, 200–219; (e) A. K. Haldar, S. Banerjee, K. Naskar, D. Kalita, N. S. Islam, S. Roy, *Exp. Parasitol.*, 495 **2009**, **122**, 145–154; (f) V. Khanna, M. Jain, M. K. Barthwal, D. Kalita, J. J. Boruah, S. P. Das, N. S. Islam, T. Ramasarma and M. Dikshit, *Pharmacol. Res.*, 2011, **64**, 274–282.
22. C. Djordjevic, N. Vuletic, B. A. Jacobs, M. Lee-Renslo and E. Sinn, *Inorg. Chem.*, 1997, **36**, 1798–1805.
23. (a) P. Hazarika, D. Kalita, S. Sarmah and N. S. Islam, *Mol. Cell Biochem.*, 2006, **284**, 39–47; (b) P. Hazarika, D. Kalita and N. S. Islam, *J. Enzy. Inhib. Med. Chem.*, 2008, **23**, 504–513.
24. C. Djordjevic, B. C. Puryear, N. Vuletic, C. J. Abelt and S. J. Sheffield, *Inorg. Chem.*, 1988, **27**, 2926–2932.
25. D. Bayot, M. Devillers and D. Peeters, *Eur. J. Inorg. Chem.*, 2005, 505 4118–4123.
26. (a) K. Nakamoto, *Infrared and Raman Spectra of Inorganic and Co-ordination Compounds*, Part B, Wiley and Sons, New York, 5th edn, 1997, pp. 62–67; (b) J. D. Gelder, K. D. Gussem, P. Vandenebeele and L. Moens, *J. Raman Spectrosc.*, 2007, **38**, 1133–1147; (c) M. Nazir and I. I. Naqvi, *Am. J. Anal. Chem.*, 2013, **4**, 134–140; (d) M. Kumar and R. A. Yadav, *Spectrochim. Acta Part A*, 2011, **79**, 1316–1325; (e) C. S. Dilip, K. J. Venkatachalam, A. P. Raj and T. Ramachandramoorthy, *Int. J. Life Sci. Pharma Res.*, 2011, **1**, 80–88; (f) J. C. Chang, L. E. Gerdorn, N. C. Baeniger and H. M. Goff, *Inorg. Chem.*, 1983, **22**, 1739–1744.
27. (a) S. T. Chow and C. A. McAuliffe, *J. inorg. nucl. Chem.*, 1975, **37**, 575 1059–1064; (b) S. Kumar and S. B. Rai, *Indian J. Pure App. Physics*, 2010, **48**, 251–255; (c) R. E. Marsh and J. Donahue, *Adv. Protein Chem.*, 1967, **22**, 235–256; (d) I. Viera, M. H. Torre, O. E. Piro, E. E. Castellano and E. J. Baran, *J. Inorg. Biochem.*, 2005, **99**, 1250–1254.
28. K. Nakamoto, *Infrared and Raman Spectra of Inorganic and Co-ordination Compounds*, Part B, Wiley and Sons, New York, 5th edn, 1997, pp. 55.
29. H. Thomadaki, A. Lymberopoulou-Karaliota and A. Maniatakou, A. Scorilas, *J. Inorg. Biochem.*, 2011, **105**, 155–163.
30. M. A. Girasolo, S. Rubino, P. Portanova, G. Calvaruso, G. Ruisi and G. Stocco, *J. Organomet. Chem.*, 2010, **695**, 609–618.
31. E. M. A. Ratilla, B. K. Scott, M. S. Moxness and N. M. Kostie, *Inorg. Chem.*, 1990, **29**, 918–926.
32. (a) D. Bayot, B. Tinant and M. Devillers, *Inorg. Chim. Acta*, 2004, **357**, 809–816; (b) L. L. G. Justino, M. L. Ramos, M. M. Caldeira and V. M. S. Gil, *Inorg. Chim. Acta*, 2003, **356**, 179–186; (c) A. C. Dengel, W. P. Griffith, R. D. Powell and A. C. Skapski, *J. Chem. Soc., Dalton Trans.*, 1987, 991–995; (d) S. E. Jacobson, R. Tang and F. Mares, *Inorg. Chem.*, 1978, **17**, 3055–3063; (e) L. Pettersson, I. Andersson and A. Gorzsas, *Coord. Chem. Rev.*, 2003, **237**, 77–87; (f) V. Conte, F. D. Furia and S. Moro, *J. Mol. Catal.*, 1994, **94**, 323–333.
33. J. J. Boruah, D. Kalita, S. P. Das, S. Paul and N. S. Islam, *Inorg. Chem.*, 2011, **50**, 8046–8062.
34. J.-C. Khan, M.-P. Halle, M.-P. SImonnln, and R. Schaal, *J. Phy. Chem.*, 1977, **81**, 587–590.
35. (a) D. Bayot, B. Tinant and M. Devillers, *Catal. Today*, 2003, **78**, 439–447; (b) J. K. Ghosh and G. V. Jere, *Thermochim. Acta*, 1988, **136**, 73–80; (c) G. V. Jere, L. Surendra and M. K. Gupta, *Thermochim. Acta*, 1983, **63**, 229–236.
36. R. G. Parr and W. Yang, *Density Functional Theory of Atoms and Molecules*, Oxford University Press, Oxford, 1989.
37. I. Bytheway and M. W. Wong, *Chem. Phys. Lett.*, 1998, **282**, 219–226.
38. (a) S. K. Maiti, S. Banerjee, A. K. Mukherjee, K. M. A. Malik and R. Bhattacharyya, *New J. Chem.*, 2005, **29**, 554–563; (b) E. Baciocchi, M. F. Gerini and A. Lapi, *J. Org. Chem.*, 2004, **69**, 3586–3589; (c) T. Patonay, W. Adam, A. Levai, P. Kover, M. Nemeth, E.-M. Peters and K. Peters, *J. Org. Chem.*, 2001, **66**, 2275–2280.
39. (a) O. A. Kholdeeva and R. I. Maksimovskaya, *J. Mol. Catal. A: Chem.*, 2007, **262**, 7–24; (b) O. A. Kholdeeva, *Eur. J. Inorg. Chem.*, 2013, 1595–1605; (c) O. A. Kholdeeva, G. M. Maksimov, R. I. Maksimovskaya, L. A. Kovaleva and M. A. Fedotov, *React. Kinet. Catal. Lett.*, 1999, **66**, 311–317; (d) H. S. Schultz, H. B. Freyermuth and S. R. Buc, *Org. Chem.*, 1963, **28**, 1140–1142; (e) O. Bortolini, F. Di Furia, G. Modena and R. Seraglia, *J. Org. Chem.* 1985, **50**, 2688–2690.
40. (a) K. Jeyakumar, R. D. Chakravarthy and D. K. Chand, *Catal. Commun.*, 2009, **10**, 1948–1951; (b) C. A. Gamelas, T. Lourenço, A. P. da Costa, A. L. Simplicio, B. Royo and C. C. Romão, *Tetrahedron Lett.*, 2008, **49**, 4708–4712; (c) A. Fuerte, M. Iglesias, F. Sánchez and A. Corma, *J. Mol. Catal. A: Chem.*, 2004, **211**, 227–235; (d) M. H. Dickman and M. T. Pope, *Chem. Rev.*, 1994, **94**, 569–584; (e) B. Tamamiand and H. Yeganeh, *Eur. Polym. J.*, 1999, **35**, 1445–1450; (f) O. Bortolini, F. Di Furia, G. Modena and R. Seraglia, *J. Org. Chem.*, 1985, **50**, 2688–2690; (g) W. Zhu, G. Zhu,

- H. Li, Y. Chao, Y. Chang, G. Chen and C. Han, *J. Mol. Catal. A: Chem.*, 2011, **347**, 8–14; (h) H. S. Schultz, H. B. Freyermuth and S. R. Buc, *J. Org. Chem.*, 1963, **28**, 1140–1142; (i) I. Sheikshoae, A. Rezaeifard, N. Monadi and S. Kaafi, *Polyhedron*, 2009, **28**, 733–738; (j) M. Bagherzadeh, L. Tahsini, R. Latifi, A. Ellern and L. K. Woo, *Inorg. Chim. Acta*, 2008, **361**, 2019–2024; (k) A. Basak, A. U. Barlan and H. Yamamoto, *Tetrahedron: Asymmetry*, 2006, **17**, 508–511; (l) K. Jeyakumar and D. K. Chand, *Tetrahedron Lett.*, 2006, **47**, 4573–4576; (m) G. P. Romanelli, P. I. Villabrilie, C. V. Cáceres, P. G. Vázquez and P. Tundo, *Catal. Commun.*, 2011, **12**, 726–730; (n) P. Tundo, G. P. Romanelli, P. G. Vázquez and F. Aricò, *Catal. Commun.*, 2010, **11**, 1181–1184.
41. (a) A. F. Ghiron and R. C. Thompson, *Inorg. Chem.*, 1989, **28**, 3647–3650; (b) K. S. Kirshenbaum and K. B. Sharpless, *J. Org. Chem.*, 1985, **50**, 1979–1982; (c) H. Mimoun, *Catal. Today*, 1987, **1**, 281–295; (d) M. Herbert, F. Montilla and A. Galindo, *J. Mol. Catal. A: Chem.*, 2011, **338**, 111–120; (e) H. Mimoun, I. Seree de Roch and L. Sajus, *Bull. Soc. Chim. Fr.*, 1969, **5**, 1481–1492; (f) K. A. Joergensen, *Chem. Rev.*, 1989, **89**, 431–458; (g) N. Gharah, S. Chakraborty, A. K. Mukherjee and R. Bhattacharyya, *Chem. Commun.*, 2004, 2630–2632, and references cited therein (h) W. R. Thiel and J. Eppinger, *Chem.–Eur. J.*, 1997, **3**, 696–705; (i) S. K. Maiti, K. M. A. Malik, S. Gupta, S. Chakraborty, A. K. Ganguly, A. K. Mukherjee and R. Bhattacharyya, *Inorg. Chem.*, 2006, **45**, 9843–9857; (j) S. K. Maiti, S. Dinda, N. Gharah and R. Bhattacharyya, *New J. Chem.*, 2006, **30**, 479–489; (k) M. S. Reynolds, S. J. Morandi, J. W. Raebiger, S. P. Melican and S. P. E. Smith, *Inorg. Chem.*, 1994, **33**, 4977–4984; (l) G. E. Meister and A. Butler, *Inorg. Chem.*, 1994, **33**, 3269–3275; (m) F. R. Sensato, R. Custodio, E. Longo, V. S. Safont and J. Andres, *J. Org. Chem.*, 2003, **68**, 5870–5874; (n) C. Djordjevic, N. Vuletic and E. Sinn, *Inorg. Chim. Acta*, 1985, **104**, L7–L9.
42. A. K. Majumdar and A.K. Mukherjee, *Anal. Chim. Acta*, 1959, **21**, 245–247.
43. M. K. Chaudhuri, S. K. Ghosh and N. S. Islam, *Inorg. Chem.*, 1985, **24**, 2706–2707.
44. M. C. Frisch, et al. Gaussian 09, revision A.1; Gaussian, Inc.: Wallingford, CT, 2009. Gaussian 09, Revision A.1, M. J. Frisch, G. W. Trucks, H. B. Schlegel, G. E. Scuseria, M. A. Robb, J. R. Cheeseman, G. Scalmani, V. Barone, B. Mennucci, G. A. Petersson, H. Nakatsuji, M. Caricato, X. Li, H. P. Hratchian, A. F. Izmaylov, J. Bloino, G. Zheng, J. L. Sonnenberg, M. Hada, M. Ehara, K. Toyota, R. Fukuda, J. Hasegawa, M. Ishida, T. Nakajima, Y. Honda, O. Kitao, H. Nakai, T. Vreven, J. A. Montgomery, Jr., J. E. Peralta, F. Ogliaro, M. Bearpark, J. J. Heyd, E. Brothers, K. N. Kudin, V. N. Staroverov, R. Kobayashi, J. Normand, K. Raghavachari, A. Rendell, J. C. Burant, S. S. Iyengar, J. Tomasi, M. Cossi, N. Rega, J. M. Millam, M. Klene, J. E. Knox, J. B. Cross, V. Bakken, C. Adamo, J. Jaramillo, R. Gomperts, R. E. Stratmann, O. Yazyev, A. J. Austin, R. Cammi, C. Pomelli, J. W. Ochterski, R. L. Martin, K. Morokuma, V. G. Zakrzewski, G. A. Voth, P. Salvador, J. J. Dannenberg, S. Dapprich, A. D. Daniels, O. Farkas, J. B. Foresman, J. V. Ortiz, J. Cioslowski, and D. J. Fox, Gaussian, Inc., Wallingford CT, 2009.